

The Effect of Swing Leg Retraction on Running Energy Efficiency

Matt Haberland, J.G.Daniël Karssen, Sangbae Kim, and Martijn Wisse

Abstract—Swing leg retraction reduces touchdown energy losses of running by decreasing foot speed at the moment of ground contact, but does the additional acceleration of the swing leg cost more energy than is saved? To determine whether swing leg retraction can increase the overall energy efficiency of running robots, we find the optimally efficient gaits of a McGeer-like runner over a range of retraction rates. Results show that overall energy usage, including that used to swing the legs, scales with energy loss at touchdown, which is minimized at the retraction rate that zeros foot tangential speed at ground contact. Other benefits of swing leg retraction, such as reduced foot slippage and damaging touchdown forces, are realized simultaneously with optimal energy efficiency.

I. INTRODUCTION

Recent advances in legged robots promise enhanced mobility of autonomous vehicles in unstructured environments [1], [2], [3]. Legged systems have the potential to outperform advanced wheeled and tracked vehicles in applications that require fast locomotion over rough terrain because discreet foot placement can reduce the effects of terrain irregularities and instabilities [4]. To simplify foot placement control, studies [5], [6] suggest influencing stance dynamics by controlling the ‘angle-of-attack’, the effective leg angle at the moment of ground contact. While it is clear that the foot placement algorithm is critical to the success of a legged robot controller, there is growing evidence that foot and leg speed at and near the moment of ground contact also plays an important role, especially as locomotion speed increases [7], [8], [9], [10].

Humans and animals exhibit a behavior called swing leg retraction (SLR) in which the airborne front leg rotates rearward before touchdown. Seyfarth et al. [7] studied the effect of SLR on running stability and stated that SLR rate ω can be tuned to improve running stability considerably. Daley et al. [8] considered the effect of SLR on injury risk, arguing that increasing ω reduces peak leg forces after a drop in terrain height.

It is also suggested that SLR can improve energy efficiency [9]. In a previous study [10], the authors showed analytically that SLR reduces touchdown energy losses of a prismatic-jointed leg by decreasing foot speed relative to the ground at the moment of contact. However, this does not necessarily

mean that overall energy efficiency is improved. For instance, additional energy required to swing the leg at the desired rate might exceed the reduction in touchdown loss. The goal of this paper is to investigate whether SLR can indeed improve the overall energy efficiency and to determine the relationship between ω and energy efficiency. We study the effect of SLR on running energy by optimizing the efficiency of simulation model gaits for a range of SLR rates.

The remainder of this paper is organized as follows: Section II describes the methods used in this study, including modeling, equations of motion generation and integration, and optimization. Section III presents the effect of SLR rate on the minimal value of an objective function, mechanical cost of transport, and two other running metrics, slip distance and peak transverse force. The paper ends with a discussion in Section IV and conclusions in Section V.

II. METHODS

A. Modeling

Running systems are inherently complex; we simplify analysis by using reduced order models and considering periodic motions, or limit cycles, of running. An ideal running model for the purpose of this study would be as simple as possible and derivable from first principles, yet capable of accurately predicting elements of dynamic behavior applicable to a range of real running machines.

The spring-mass, or Spring Loaded Inverted Pendulum (SLIP), model featured in [6] is the most popular model for running analysis due to its simplicity. With tuned parameters, it can accurately predict data recorded from running humans, such as body center of mass traces. However, the SLIP model is energy-conservative due to the massless spring leg. Thus, it is unsuitable for analysis of energy efficiency.

The running model proposed by McGeer in [11] has legs with distributed mass that can yield non-zero impact losses, which makes the model suitable for analyzing energy efficiency. In this study, we use a variation of the McGeer running model consisting of a point mass body with two rigid legs of distributed mass, each connected by a massless spring to a massless point foot. A torque actuator between the legs provides energy and control as the model runs over a flat, level surface.

B. Equations of Motion

The three distinct phases of motion of the model are shown in Figure 1: flight, touchdown, and stance. The equations of motion for each phase are derived using Lagrangian mechanics. During flight and touchdown there is relative velocity between the front foot and the ground, so x , y , θ_1 ,

M. Haberland and S. Kim are funded by the Defense Advanced Research Project Agency and are with the Biomimetic Robotics Laboratory, Department of Mechanical Engineering, Massachusetts Institute of Technology, 77 Massachusetts Avenue, Cambridge, Massachusetts, USA mdhaber@mit.edu.

J.G.D. Karssen and M. Wisse are funded by the Dutch Technology Foundation STW and are with the Delft Biorobotics Laboratory, Department of BioMechanical Engineering, Faculty of Mechanical Engineering, Delft University of Technology, 2628 CD, Delft, The Netherlands j.g.d.karssen@tudelft.nl.

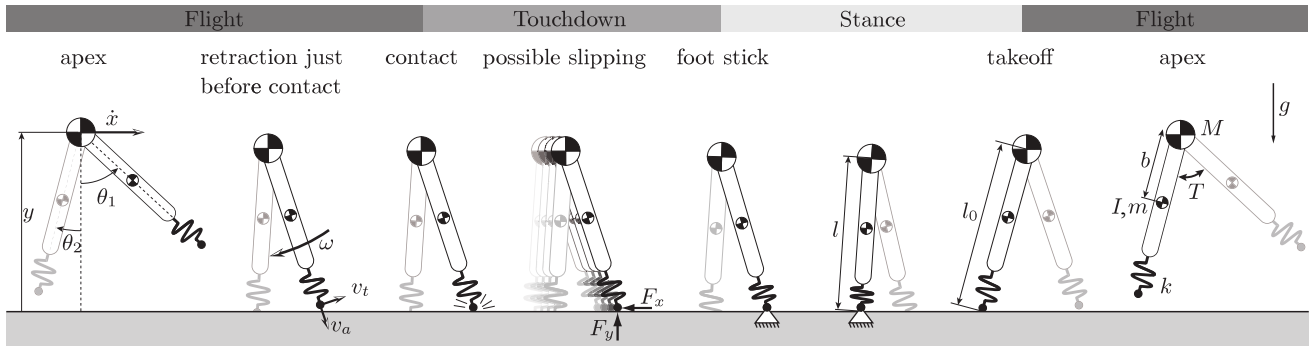


Fig. 1. Modified McGeer running model with point foot and hip torque T . The swing leg rotates with retraction rate ω and the foot has tangential speed v_t immediately prior to contact with the ground. After contact, the foot can slip due to finite friction. When the foot does come to rest with respect to the ground, it acts as a pivot point until the leg spring free length l_0 is reached and takeoff occurs.

and θ_2 are used as the generalized coordinates. While both of these phases have four degrees of freedom, interaction between the front foot and the ground must be modeled during touchdown with generalized forces. Friction is assumed to be Coulombic while there is relative motion between the front foot and the ground; collision of the other foot with the ground is ignored for simplicity. Once the front foot reaches zero velocity with respect to the ground, it is assumed to stick, and the stance phase begins. During stance, the three generalized coordinates l , θ_1 , and θ_2 are sufficient. Interaction with the ground enters these equations in the form of a spring potential function. Gravity is included in all phases through a potential function. Due to the complexity of the resulting equations, the authors gained no insight from “hand” analysis. Instead, integration is performed using MATLAB’s `ode45()` function with absolute and relative tolerances less than or equal to 10^{-9} .

1) Touchdown Ground-Leg Interaction: It is important to model the ground-leg interaction carefully, as this is a primary source of energy loss in the model. Several options were considered for modeling this interaction from the moment of contact until the foot halts with respect to the ground.

a) Impulsive Collision: The simplest option would be to follow [11] and assume that the foot sticks to the point of contact at the instant of touchdown. The state after impact can be calculated by assuming an impulsive collision and solving momentum balance equations. In most situations of interest, however, this calculation results in an impulse applied to the foot with a component directed toward the floor. This is physically realizable only if the floor can pull on the leg, which is not the case in normal running. Thus, the impulsive collision model is deemed unacceptable for this study.

b) Semi-Impulsive Collision: To address the deficiency of the impulsive collision model, we can formulate a semi-impulsive collision model that is consistent with a floor that cannot pull. In this model, it is assumed that constant external forces due to gravity and the floor act for a short period of time Δt , during which position variables remain fixed but speed variables change rapidly. While three momentum

balance equations govern this change, we are left with four unknowns: the normal force of the floor, Δt , and two final speeds. However, as it is unclear which of several reasonable additional relationships will define the most accurate unique solution, we seek a more conventional, less subjective model.

c) Coulombic Friction: A third possibility is to instantaneously halt motion of the foot along the floor surface normal, but allow it to slip horizontally and include Coulombic friction in the equations of motion. The vertical component of ground reaction force F_y is a function of spring compression and leg angle during touchdown; it is found by balancing forces on the massless spring. Then the horizontal friction force is simply $F_x = \mu F_y$ acting in the direction that opposes the foot’s horizontal travel. We choose this approach because this method allows us to study foot slip distance with the choice of a single parameter, friction coefficient μ .

2) Takeoff Ground-Leg Interaction: The ground-leg interaction at takeoff is also important as it determines when the transition to flight occurs. Before the spring reaches its free length l_0 at the end of stance, the horizontal component of the ground reaction force F_x is observed in Figure 2 to exceed the Coulombic theoretical maximum of μF_y . The simple approach is to ignore the discrepancy and continue integrating the stance equations of motion until the spring reaches its free length. A more consistent way to treat this would be to transition to the equations of motion used during touchdown, which enforce the horizontal force constraint $F_x = \mu F_y$. All integration schemes tested encountered significant numerical difficulties with this approach: because the horizontal velocity of the foot is zero when integration of these equations begins, the horizontal velocity of the foot oscillates between positive and negative values as the horizontal force jumps instantaneously to oppose the motion, and integration stalls. However, as the duration of the discrepancy in the simple approach is very short and the magnitudes of the forces involved are very small, the error in total impulse is considered negligible. Thus, we assume that once the foot speed reaches zero, it remains zero and the foot acts as a pivot until the spring reaches its free length l_0 .

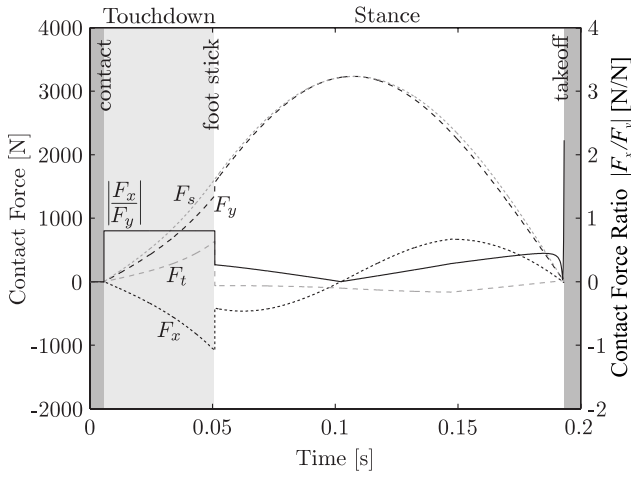


Fig. 2. Example of ground reaction force components as functions of time, from touchdown to takeoff. Note that ratio $\frac{F_x}{F_y}$ briefly exceeds the chosen maximum $\mu = 0.8$ just before takeoff. However due to the low force magnitudes during this short time, the total error in impulse is neglected for simplicity.

C. Optimization

In this study, we seek to optimize limit cycle energy efficiency. We quantify the energy efficiency as the mechanical cost of transport c_{mt} , which is the energy consumed normalized by the product of weight and distance travelled [12]. The energy consumed is taken as the integral of the absolute mechanical power of the torque actuator $|T \cdot \dot{\phi}|$ plus a fraction $(1 - \eta)$ of the positive power of the leg spring $k \cdot (l - l_0) \cdot \dot{l}$, $\dot{l} > 0$. This results in the following objective function,

$$c_{mt} = \frac{\int_0^{t_{step}} [|T \cdot \dot{\phi}| + (1 - \eta) \cdot k \cdot (l - l_0) \cdot \dot{l}] dt}{(M + 2m) \cdot g \cdot x_{step}}, \quad (1)$$

in which t_{step} is the duration of a step, x_{step} is the distance traveled in one step, $\dot{\phi}$ is the relative angular rate between the legs, T is the hip torque, and other symbols are defined in Table I. The leg spring efficiency η is initially taken to be 100%, and thus spring work does not enter the calculation, however we will relax this assumption in III-C.

The single-shooting technique presented in [13] is used to formulate a nonlinear programming problem to minimize c_{mt} , which is then solved using the active set method of MATLAB's `fmincon()` with all tolerances set to 10^{-6} . The initial leg states and hip actuation pattern, parameterized as a piecewise linear torque profile connecting 10 control points, are optimized to minimize c_{mt} for a fixed body apex horizontal speed, body apex height, and set of physical parameters.

Optimization is initially seeded with a passive bouncing motion, then iterated from a randomly perturbed variant of the most efficient solution yet found. After hundreds of iterations with seed perturbation values ranging over several binary orders of magnitude, optimization proceeds with ω constrained in $1/10$ rad/s increments over a range. Using the

TABLE I
MODEL PARAMETER VALUES USED IN ALL CALCULATIONS
(UNLESS VARIATIONS ARE EXPLICITLY NOTED):

Parameter	Symbol	Value	Unit
Body Mass	M	64	[kg]
Leg Mass	m	8	[kg]
Leg Inertia about CoM	I	$\frac{8}{12}$	[kg m ²]
Nominal Leg Length	l_0	1.0	[m]
Center of Mass Location	b	0.5	[m]
Gravitational Acceleration	g	9.81	[m/s ²]
Leg Stiffness	k	20000	[N/m]
Friction Coefficient	μ	0.8	[N/N]
Body Apex Height	y_0	1.0	[m]
Body Apex Horizontal Velocity	\dot{x}_0	5.0	[m/s]

previous solution as a seed, the gait resulting in the locally minimal objective function value is found for each value of ω . The procedure is performed using the parameters of Table I and repeated for several body apex horizontal speeds, body apex heights, and leg masses. Example optimal torque profiles for several swing leg retraction rates are shown in Figure 3.

III. RESULTS

A. Basic Trends

Figure 4 shows energy expenditures and the corresponding foot tangential speed v_t (magnitude of the velocity of the foot in the direction perpendicular to the leg at the instant of touchdown, as illustrated in Figure 1) as functions of ω for the parameters in Table I. The minimum of the touchdown loss curve and the zero of the foot tangential speed curve occur at the same retraction rate, as anticipated by analysis presented in [10]. What is significant and non-intuitive is

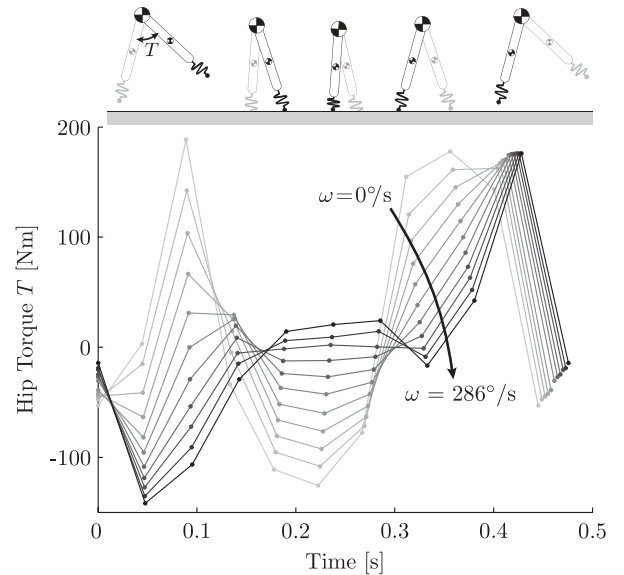


Fig. 3. Torque profile of minimal c_{mt} limit cycle for several values of SLR rate ω .

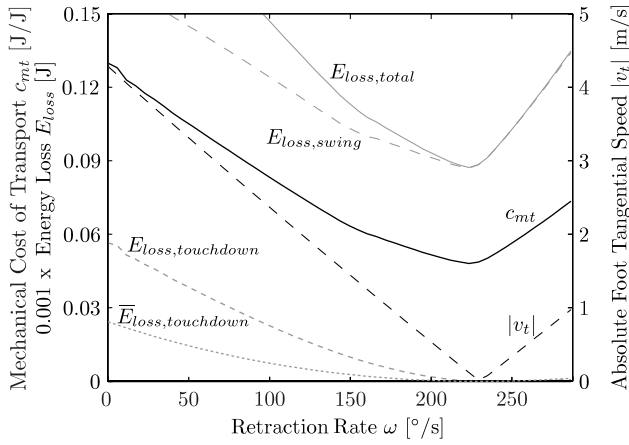


Fig. 4. Minimal c_{mt} with corresponding energy expenditures and foot tangential speed $|v_t|$ as functions of SLR rate ω . Touchdown loss $E_{loss,touchdown}$ is the energy expenditure associated with touchdown. Swing loss $E_{loss,swing}$ is the work required to swing the legs. Their sum $E_{loss,total}$, is the total energy consumed by the actuator over a limit cycle. The quantitative difference between the numerically integrated value of touchdown loss $E_{loss,touchdown}$ and the analytical approximation $\bar{E}_{loss,touchdown}$ of [10] is due to the difference in models: the analytical approximation is derived assuming the impulsive collision of II-B.1.a; the numerically integrated value uses the friction model of II-B.1.c. However, there is clear qualitative agreement: minima of all these curves occur at or near the retraction rate of zero foot tangential speed.

that the total work required to drive the legs $E_{loss,swing}$ corresponds closely with the touchdown loss. As a result, the minimum of the c_{mt} curve and the zero of the foot tangential speed curve occur at nearly the same retraction rate. This is typical for all parameters sets studied.

B. Parameter Variation

Figures 5, 6, and 7 show the minimal c_{mt} as a function of ω for several body apex heights, body apex horizontal speeds, and leg masses. The minima of all these curves closely correspond with a foot tangential speed of zero at the instant of contact. This indicates that the SLR rate resulting in zero foot tangential speed yields nearly optimal energy efficiency independent of model parameters.

C. Spring Inefficiency

In the optimization presented above, it is assumed that the leg spring is ideal with no energy loss. We relax this assumption by varying spring efficiency η . Figure 8 shows that c_{mt} increases as η decreases, as might be expected. While optimal retraction rate drifts from that corresponding with $v_t = 0$ as η decreases, minimal c_{mt} is found at a relatively high retraction rate for all η .

D. Other Benefits

The reduced foot speed due to SLR benefits more than energy efficiency; decreased slip distance and lower peak transverse force are apparent in Figure 9:

1) *Slip Distance*: This is the distance that the foot slides during touchdown, from the instant of contact until the foot speed reaches zero.

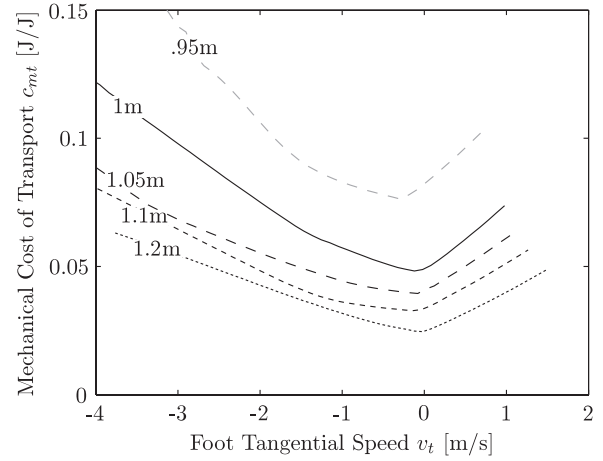


Fig. 5. Minimal c_{mt} as function of v_t for several body apex heights. The minima of all these curves lie at approximately zero foot tangential speed.

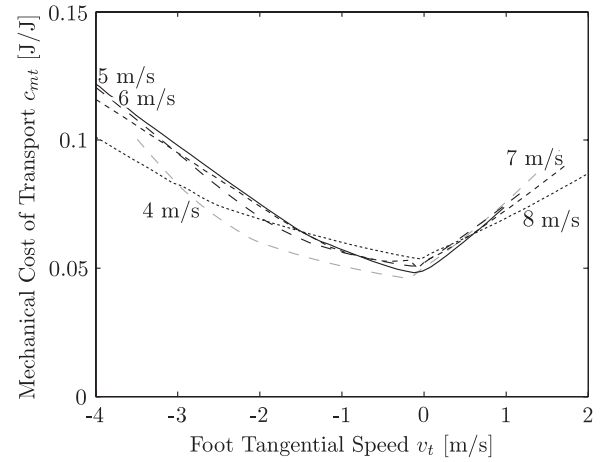


Fig. 6. Minimal c_{mt} as function of v_t for several body apex horizontal speeds. The minima of all these curves lie at approximately zero foot tangential speed.

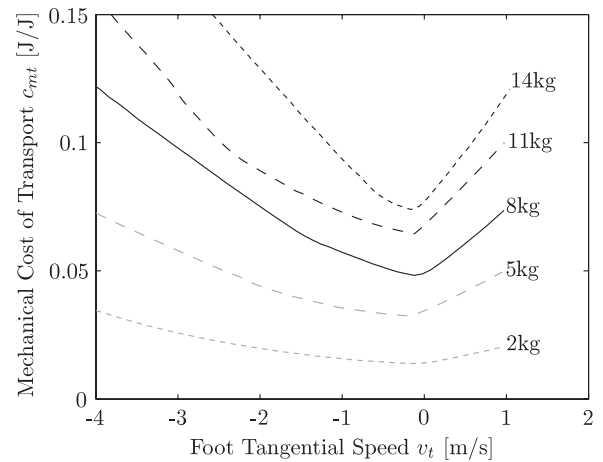


Fig. 7. Minimal c_{mt} as function of v_t for several leg masses. The minima of all these curves lie at approximately zero foot tangential speed.

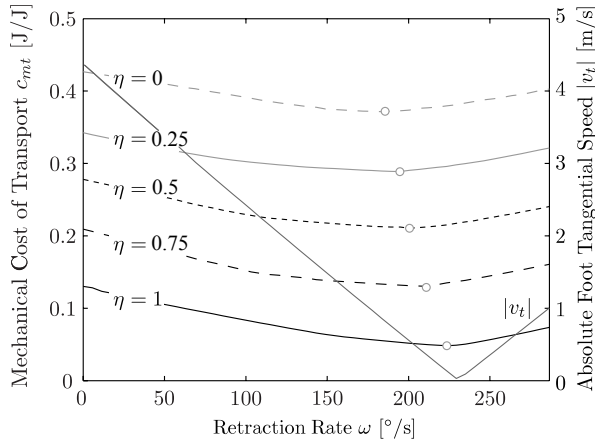


Fig. 8. Minimal c_{mt} as function of ω for several values of spring efficiency η . Energy lost due to spring inefficiency is assumed to be replaced such that the resulting force/displacement profile is that of a lossless spring, $F = k(l - l_0)$. The dynamics are unchanged, but replaced energy is included in calculation of c_{mt} . The minima of these curves do not all correspond with foot tangential speed $v_t = 0$, but all are still at relatively high retraction rates.

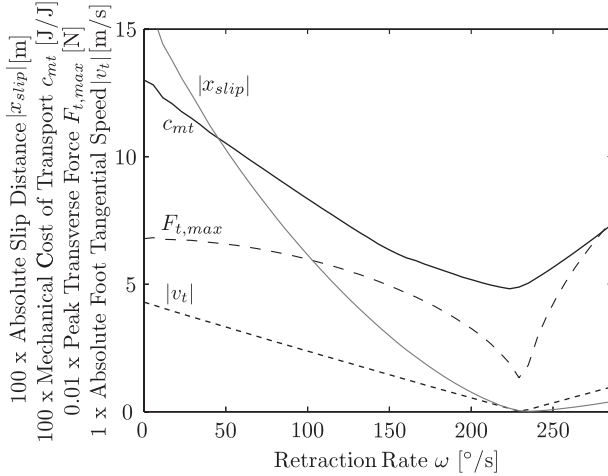


Fig. 9. Minimal c_{mt} and corresponding foot tangential speed, slip distance, and peak transverse force as functions of SLR rate ω . The minima of all these curves occur at or near the retraction rate ω of zero foot tangential speed.

2) *Peak Transverse Force*: This is the peak magnitude of the component of ground reaction force perpendicular to the leg. Note that for many running robots, and especially for those with prismatic legs such as in [14], the peak transverse force may serve as a good measure of damage risk due to the potentially high resulting bending moments.

The minima of both of these curves occur at nearly the same retraction rate as minimum c_{mt} . This is typical of all parameter sets studied.

IV. DISCUSSION

The motivation of this study was to understand the effect of swing leg retraction on energy efficiency. We hypothesized that for a given running speed, swing leg retraction would decrease the foot speed with respect to the ground and thereby reduce the energy loss due to touchdown. This is

confirmed in Figure 4 in that the minimum of the touchdown loss curve occurs at a nonzero SLR rate ω . We further hypothesized that swing leg retraction would permit more efficient running overall, despite the possibility that increased retraction rate might require more energy to swing the leg over the course of a cycle. This hypothesis is also confirmed in Figure 4 in that the minimum of the c_{mt} curve occurs at a nonzero ω . In fact, the same conclusion holds even when positive work done by the leg spring is included in the calculation for c_{mt} ; when considering three of the most significant energy inefficiencies of running (touchdown loss, leg swinging, and leg axial impulse application), the most efficient running is realized with a nonzero ω . This is demonstrated in Figure 8 in that the curves for c_{mt} calculated for all spring efficiencies have minima at a nonzero ω .

Note in Figure 4, however, that the touchdown loss $E_{loss,touchdown}$ is only a portion of the total energy loss $E_{loss,total}$. This simulation study shows that a substantial portion of the energy expenditure, the swing loss $E_{loss,swing}$, is dedicated just to moving the legs. Surprisingly, these swing losses are also minimal near the SLR rate for which touchdown losses are minimal. These swing losses are precisely the reason that analytical calculations are insufficient and this numerical study is needed: while intuition and hypotheses that SLR can increase running efficiency are correct, the intuitive reasoning for this effect may not provide a complete explanation. Further analysis is needed to explain the shape of the swing loss curve.

Based on analytical results presented in [10], we expected the minimum of the touchdown loss curve to correspond with a near-zero foot tangential speed. We hypothesized that the minimum of the c_{mt} curve would also occur with a near-zero foot tangential speed. These expectations were confirmed for a range of body apex heights, body apex horizontal speeds, and leg masses as shown in Figures 5, 6, and 7, respectively.

It is interesting to note that other hypothesized benefits of swing leg retraction, namely reduced foot slippage and peak transverse forces, are also realized when optimizing the limit cycle for minimal c_{mt} . This is shown in Figure 9 in that the minima of the slip distance and peak transverse force curves occur very near the retraction rate for zero foot tangential speed and minimal c_{mt} . While this alone does not prove an inherent relationship between these other benefits and zero foot tangential speed, it is useful information for the design of a robot controller: the retraction rate for minimal c_{mt} also results in relatively low slippage and transverse forces.

A. Future Works

1) *More parameter variation*: Additional parameter variation could strengthen the claims of this paper by showing them to be true under a wider variety of conditions. In particular, we would like to study even higher horizontal speeds because we are most interested in the challenges associated with high speed running.

2) *Additional Model Detail*: Another valuable extension to the current work would be to perform the analysis using a more detailed model. Specifically, while a point body

mass and torque acting between two legs could accurately represent a running robot configured like the Cornell Ranger walking robot of [15], the addition of a massive torso could show that the conclusions of this paper apply to a greater variety of robots in which torque is applied between the body and each of two legs independently. Another important change would be to permit active control of the push-off. Analysis done including spring work in the c_{mt} calculation suggests that energy expenditure due to push-off would not change the conclusions significantly, but a controllable telescoping actuator should be added to the model to verify this. Then, replacement of the prismatic leg joint with a rotating knee would make the analysis applicable to a different class of running robots. Compression of a kneed leg at impact causes angular accelerations of the leg segments in opposite directions; this and knee rotation prior to impact affect touchdown losses. The authors plan to study a kneed simulation model and robotic hardware in the near future.

3) *Stability/Disturbance Rejection Analysis*: While the trends of this paper have only been shown explicitly for limit cycle running without disturbances, it is likely that they hold even in the presence of small, isolated disturbances. For instance, nonlinear predictive model control [16] stabilizes trajectories by ‘online replanning’, that is, repeatedly optimizing the trajectory from the current state using the last control trajectory as the seed. During this study, small changes in initial state have consistently yielded small changes in trajectory, and thus small changes in energy efficiency. Thus, while the conclusions have been drawn for limit cycle running, it is unlikely that they are restricted to limit cycle running. Still, this should be explicitly verified.

V. CONCLUSION

The current work has important implications for the design of running robot control systems: not only is the effective leg angle at touchdown important, so is the rate of change of leg angle at touchdown. In addition to the stability implications of swing leg retraction, the designer must consider the effect of swing leg retraction on energy efficiency, damaging peak forces, and footing security. Swing leg retraction is recommended as an element of any control strategy for running robots with compliant, prismatic legs in order to maximize energy efficiency. The optimum SLR rate for maximum

energy efficiency also results in good footing security and low peak transverse leg forces. Furthermore, this optimum SLR rate is strongly correlated, for various limit cycles and model parameters, to zero foot tangential speed.

REFERENCES

- [1] R. Playter, M. Buehler, and M. Raibert, “Bigdog,” G. R. Gerhart, C. M. Shoemaker, and D. W. Gage, Eds., vol. 6230, no. 1. SPIE, 2006, p. 62302O. [Online]. Available: <http://link.aip.org/link/?PSI/6230/62302O/1>
- [2] U. Saranlı, M. Buehler, and D. E. Koditschek, “RHex: A Simple and Highly Mobile Hexapod Robot,” *The International Journal of Robotics Research*, vol. 20, no. 7, pp. 616–631, 2001. [Online]. Available: <http://ijr.sagepub.com/content/20/7/616.abstract>
- [3] S. Kim, J. E. Clark, and M. R. Cutkosky, “iSprawl: Design and Tuning for High-speed Autonomous Open-loop Running,” *The International Journal of Robotics Research*, vol. 25, no. 9, pp. 903–912, 2006. [Online]. Available: <http://ijr.sagepub.com/content/25/9/903.abstract>
- [4] M. H. Raibert, “Legged robots,” *Commun. ACM*, vol. 29, no. 6, pp. 499–514, 1986.
- [5] A. Seyfarth, H. Geyer, M. Gunther, and R. Blickhan, “A movement criterion for running,” *Journal of Biomechanics*, vol. 35, pp. 649–655(7), May 2002. [Online]. Available: <http://www.ingentaconnect.com/content/els/00219290/2002/00000035/00000005/art00245>
- [6] R. Blickhan, “The spring-mass model for running and hopping,” *Journal of Biomechanics*, vol. 22, no. 11-12, pp. 1217–1227, 1989.
- [7] A. Seyfarth, H. Geyer, and H. Herr, “Swing-leg retraction: a simple control model for stable running,” *Journal of Experimental Biology*, vol. 206, no. 15, p. 2547, 2003.
- [8] M. Daley and J. Usherwood, “Two explanations for the compliant running paradox: reduced work of bouncing viscera and increased stability in uneven terrain,” *Biology Letters*, vol. 6, no. 3, p. 418, 2010.
- [9] M. H. Raibert, *Legged robots that balance*. Cambridge, MA, USA: Massachusetts Institute of Technology, 1986.
- [10] J. G. D. Karssen, M. Haberland, M. Wisse, and S. Kim, “The optimal swing-leg retraction rate for running,” in *IEEE International Conference on Robotics and Automation*, 2011, accepted for publication.
- [11] T. McGeer, “Passive bipedal running,” *Proc. R. Soc. B*, vol. 240, no. 1297, 1997.
- [12] S. Collins, A. Ruina, R. Tedrake, and M. Wisse, “Efficient Bipedal Robots Based on Passive-Dynamic Walkers,” *Science*, vol. 307, no. 5712, pp. 1082–1085, 2005. [Online]. Available: <http://www.sciencemag.org/cgi/content/abstract/307/5712/1082>
- [13] M. Srinivasan, “Trajectory optimization, a brief introduction,” Powerpoint Presentation at Dynamic Walking Conference, 2010.
- [14] R. Playter and M. Raibert, “Control of a biped somersault in 3d,” vol. 1, jul. 1992, pp. 582–589.
- [15] J. G. D. Karssen, “Design and construction of the cornell ranger, a world record distance walking robot,” 2007. [Online]. Available: http://ruina.tam.cornell.edu/research/topics/locomotion_and_robotics/ranger/CornellRangerKarssen.v22.pdf
- [16] F. Allgöwer and A. Zheng, *Nonlinear model predictive control*. Boston, MA, USA: Birkhäuser, 2000.